BMC Cancer

RESEARCH

Open Access

The staining results of early gastric cancer by indigo carmine chromoendoscopy associated with histological structure: a retrospective study

Xiaosa Jiang[1†], Lingzhi Qin[1†], Yujie Hao[1], Qian Yang[1], Yueqin Zheng[1], Baicang Zou[1], Lei Dong[1], Na Liu[1], Jinhai Wang[1*] and Bin Qin[1*]

Abstract

Background At present, conventional endoscopy and chromoendoscopy using indigo carmine (IC) is a very useful method to determine the demarcation line (DL) of early gastric cancer lesions, but it is not suitable for all lesions.

Aims This study aimed to determine the applicable conditions for IC chromoendoscopy.

Methods We retrospectively evaluated 187 lesions in 181 patients who had an endoscopic diagnosis of EGC and were treated with endoscopic submucosal dissection (ESD). According to the existence of the DL between the lesion mucosa and normal mucosa with IC chromoendoscopy, the lesions were divided into two groups: clear group and unclear group. Clinicopathological characteristics were evaluated in each group. From January 2022 to March 2023, the postoperative pathological sections of 19 lesions (81 slices) in the clear group and 19 lesions (80 slices) in unclear group were scanned with high definition, and the crypt structure between the two groups was evaluated.

Results There was no significant difference in clinical factors between the clear group and unclear group. There were significant differences in crypt area, crypt length, and crypt opening diameter between the two groups. In the clear group, there were significant differences in crypt area, crypt length, and crypt opening diameter between the normal area and cancer area, but there was no significant difference in the unclear group.

Conclusions The margins of lesions with fused or absent crypt structures, a small crypt area, a short crypt length, and a short crypt opening diameter can be easily determined with IC chromoendoscopy.

Keywords Early gastric cancer, Endoscopic submucosal dissection, Indigo Carmine, Chromoendoscopy

†Xiaosa Jiang and Lingzhi Qin contributed equally to this work.

*Correspondence:
Jinhai Wang
jinhaiwang@hotmail.com
Bin Qin
qinbin16@163.com
[1]Department of Gastroenterology, Second Affiliated Hospital, Xi'an Jiaotong University, Xi'an 710004, China

Introduction

Endoscopic submucosal dissection (ESD) has been widely accepted for the resection of early gastric cancer (EGC) with a low risk of lymph node metastasis due to its advantages of minimal trauma, total resection, and good prognosis. During this procedure, the accurate determination of the tumor edge is a necessary condition to avoid the residual margin and achieve complete resection [1, 2].

Recently, for tumor border determination, we have mainly relied on white light endoscopy (WLE) combined with chromoendoscopy and magnifying endoscopy with narrowband imaging (ME-NBI). Chromoendoscopy is more widely applied in clinics than ME-NBI due to its simple operation and lack of need for additional endoscopic equipment [3]. Indigo carmine, the representative, can clearly display the morphological characteristics of gastric mucosal microlesions and delineate the demarcation line of the lesions by increasing the contrast between normal and pathological areas. However, this method is not effective for all early gastric cancer lesions. It has been reported that approximately 20% of lesion boundaries cannot be clearly shown after staining [4]. In such cases, ME-NBI may be an effective remedial measure, but because it requires special endoscopic equipment, it is bound to increase the risk of secondary entry. Therefore, it is crucially important to select the appropriate examination method to accurately evaluate the lesion before the operation, and it also requires us to clarify the applicable conditions of each method.

In addition, the IC-staining mechanism is mainly due to the fact that the gastric mucosal epithelium cannot absorb IC, thus allowing it to be deposited into the depressed structures of the mucosal surface [5]. Therefore, the staining effect of IC chromoendoscopy should be inextricably linked to the microstructure of the mucosal surface. However, this has not been confirmed by previous studies. Given this background, the present study aimed to determine the applicable conditions of IC to identify the demarcation lines of early gastric cancer lesions on the one hand and to explore the relationship between the surface microstructure of mucosa and the effect of indigo carmine staining on the other hand.

Materials and methods

Participants

Patients with EGC treated in the Second Affiliated Hospital of Xi'an Jiaotong University from January 2015 to March 2023 who met the following inclusion and exclusion criteria were included in the study. The inclusion criteria for this study were as follows: ① Patients diagnosed with EGC or high-grade intraepithelial neoplasia according to WHO histological diagnostic criteria; ② Patients who underwent ESD without any antitumor therapy before the operation; ③ IC chromoendoscopy was used to determine the horizontal border of the lesion before the operation; ④ Lump resection. The exclusion criteria were as follows: ① Patients diagnosed with recurrent gastric cancer or gastric stump cancer; ② The endoscopic picture and image data were unclear or missing; ③ The clinical pathological data were incomplete. All ESD procedures in this study were performed by two physicians with over 10 years of endoscopic experience. This study was approved by the Medical Ethics Committee of the Second Affiliated Hospital of Xi'an Jiaotong University (Approval No. 2021196). Since the study neither contains personal information nor involves commercial interests, the requirement for informed consent was waived by the committee during the ethical application process.

Data collection

The following data were collected: gender, age, height, weight, history of smoking and drinking, past history, tumor location, tumor diameter, macroscopic type, depth of invasion, histopathology, lesion characteristics, atrophy, intestinal metaplasia, tumor markers (Carcinoembryonic antigen, CEA; Carbohydrate antigen199, CA199; Carbohydrate antigen724, CA724), lymphatic and vascular invasion.

Definition

Based on the visibility of the demarcation line (DL) after indigo carmine staining, the lesions were categorized into a clear group and an unclear group. The determination of DL required meeting two criteria: the absence of regular features in the background mucosa and the detection of an irregular surface structure within the marginal line [6]. The clear group was defined by a distinct DL between the normal mucosa and the lesion mucosa approximately 2–3 min after indigo carmine staining (Fig. 1a and b). Conversely, the unclear group was characterized by the absence of a discernible DL between the normal mucosa and the pathological mucosa following staining (Fig. 1c and d) [7]. For accurate diagnosis of the lesion boundary in the unclear group, ME-NBI was employed. The margins were determined based on: (1) abrupt changes in the regular microvascular and microsurface patterns in the normal mucosa, and (2) detection of irregular microvascular or microsurface patterns inside the demarcation line [8, 9]. Once the lesion boundary was established, electrocoagulation marking was performed with an electrotome approximately 5 mm from the lesion boundary, defining the precise scope for lesion resection. The staining results were determined by an experienced endoscopic physician without knowing the histological results of the biopsy before the operation. The general classification of lesions was performed according to the 2005 Paris classification standard [10]. According to the WHO classification standard of digestive system tumors

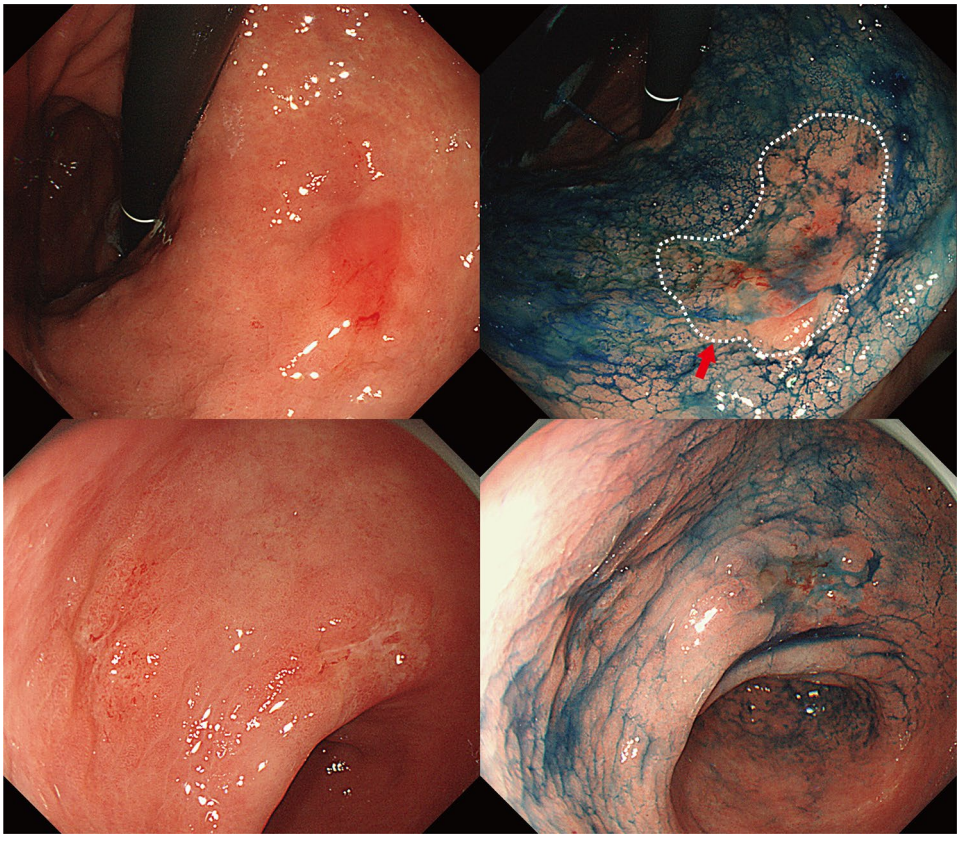

Fig. 1 Example cases of border distinction on WLE and IC chromoendoscopy. **a**, **b** A case of a differentiated EGC lesion. **a** On WLE, a flat lesion with central redness and peripheral roughness was seen at the gastric body. Its border appeared indistinct. **b** After AI chromoendoscopy, the border of the lesion became clear. The dotted white box shown by the red arrow is the boundary of the lesion. **c**, **d** A case of multiple undifferentiated EGC lesions. **c** On WLE, a superficial depressed lesion was shown at the gastric antrum. Its border appeared indistinct. **d** After AI chromoendoscopy, the border of the lesion became unclear

[11], the lesions were divided into the differentiated type and undifferentiated type. The diagnosis of atrophy and intestinal metaplasia (IM) was based on the pathological results.

Histological measurement

From January 2022 to March 2023, a total of 19 lesions were included in the clear group and 5 lesions were included in the unclear group. In order to make the two groups comparable, 14 cases of unclear lesions matched with clear lesions before 2022 were also included in the unclear group. All the obtained pathological sections stained by hematoxylin and eosin (HE) were scanned with Nano Zoomer (Hamamatsu Photonics, Shizuoka, Japan). The slides were viewed with NDP View 2 software (Hamamatsu Photonics, Shizuoka, Japan), and the parts without tissue breakage, deletion, or overlap were collected under a 5X visual field (Fig. 2a). The collected images were sequentially imported into ImageJ software(NIH, Bethesda, USA), and the following histological data were measured with reference to the experience of Kenta Chuman et al. [12]. ①crypt area, the area occupied by each crypt opening (Fig. 2b); ②crypt length, the distance from the center of the crypt opening to the deepest part of the crypt (Fig. 2c); ③crypt opening diameter, the distance across the crypt opening (Fig. 2d); ④intercrypt distance, the distance between crypts (Fig. 2e). Histological data were measured by an experienced pathologist who was blinded to the endoscopy results. After reading and analyzing all the pathological pictures, it was found that the changes in crypt structure were mainly manifested in three types: regular crypts (Fig. 2f), fused crypts (Fig. 2g), and absent crypts (Fig. 2h). The crypt type of the lesion was determined by more than half of the structural changes in the whole pathological section.

Statistical analysis

Statistical analysis was performed with SPSS 17.0 software (SPSS Inc., Chicago, IL, USA). The counting data between the clear group and unclear group are expressed by the constituent ratio; differences in lesion-related factors were analyzed with the chi-square test or Fisher's exact probability method. Histological-related meteorological data are expressed as $\bar{x} \pm s$ and a t-test was used

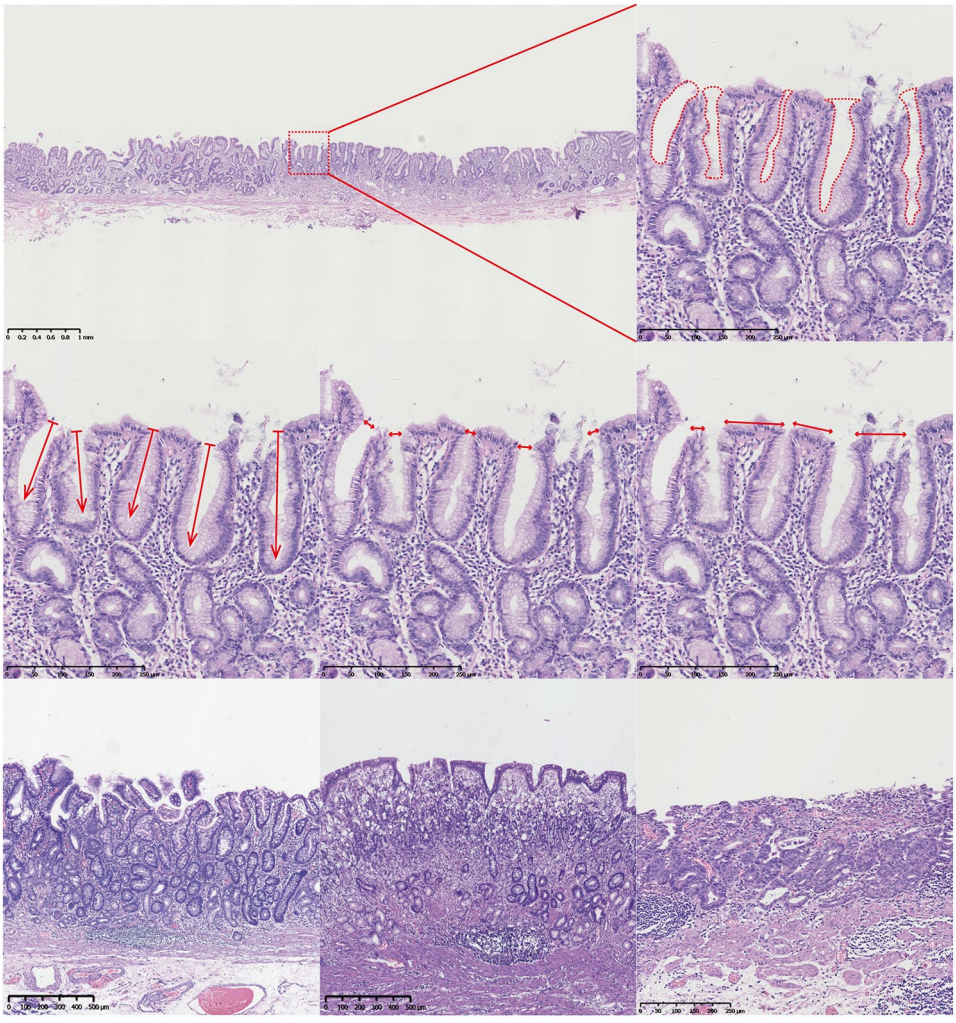

Fig. 2 **a** Pathological images of the HE-stained lesions. Scale bar, 1 mm; **b** Enlarged image of the red box in a; Scale bar, 250 μm; The red dotted line indicates the area of the crypt; **c** The red arrow indicates the crypt length; **d** The red double arrow indicates the diameter of the crypt opening; **e** The red double arrows indicate the distance between crypts; **f** Regular crypt; **g** Fused crypt; **h** Absent crypt

Table 1 Clinical characteristics of patients with early gastric cancer

Characteristics	**Total study population, mean ± SD**
Age (yr)	62.80 ± 8.57
BMI (Kg/m^2)	22.78 ± 3.25
Characteristics	Total study population, n (%)
Male	143 (79.01%)
Female	38 (20.99%)
Smoking history	67 (37.02%)
Drinking history	33 (18.23%)
Hypertension	53 (29.28%)
Diabetes	21 (11.60%)
Cardiovascular and cerebrovascular diseases	21 (11.60%)

Note SD, standard deviation

to evaluate the difference between the two groups. For groups that did not satisfy a normal distribution, appropriate non-parametric tests were employed. One-way analysis was used to analyze differences between more than two groups. $P < 0.05$ was considered statistically significant.

Results

Patient characteristics and lesion-related characteristics

A total of 181 EGC patients were included in the study. The baseline characteristics of all participants are shown in Table 1. A total of 187 lesions were found in 181 EGC patients, of which 34.22% were located in the gastric antrum. The majority of lesions were ≤20 mm in size (127 cases). Lesion infiltration was limited to the mucosal layer in 172 cases. Histopathologically, 173 tumors were differentiated type and 14 were undifferentiated type (Table 2).

Table 2 Characteristics of 187 EGC lesions and comparison of related factors between the clear group and unclear group

Characteristics	*n* (%)	Clear group *n* = 151	Unclear group *n* = 36	*P* value
Tumor location				0.3914
Cardia	43 (22.99%)	36	7	
Fundus	10 (5.35%)	7	3	
Antrum	64 (34.22%)	48	16	
Angle	26 (13.9%)	21	5	
Body	44 (23.53%)	39	5	
Tumor diameter				0.8451
≤ 20 mm	127 (67.91%)	103	24	
> 20 mm	60 (32.09%)	48	12	
Macroscopic type				0.532
I/IIa	77 (41.18%)	65	12	
IIb	38 (20.32%)	29	9	
IIc/III	72 (38.5%)	57	15	
Depth of invasion				0.7397
Mucosa	172 (91.98%)	138	34	
Submucosa	15 (8.02%)	13	2	
Histopathology				0.1502
Differentiated	173 (92.51%)	142	31	
Undifferentiated	14 (7.49%)	9	5	
Lesion characters				
Margin elevation	14 (7.49%)	11	3	0.7351
Remarkable redness	103 (55.08%)	80	23	0.2671
Uneven surface	112 (59.89%)	87	25	0.2563
Ulcer	11 (5.88%)	8	3	0.4454
With atrophy	69 (36.9%)	56	13	> 0.9999
With IM	97 (51.87%)	80	17	0.5807
CEA(+)	11 (5.88%)	10	1	0.6939
CA199(+)	5 (2.67%)	4	1	> 0.9999
CA724(+)	26 (13.9%)	23	3	0.4217

Factors associated with IC staining result

The border of the lesion was clear in 57.75% (108/187) of cases with white light endoscopy and in 80.75% (151/187) of cases with IC chromoendoscopy ($P<0.001$). Based on the postoperative pathological results, 94.12% (176/187) of the lesions were completely resected, and 11 cases had residual margins. The 187 included lesions were divided into two groups according to the effect of indigo carmine staining, of which 151 cases were classified into the clear group and 36 cases into the unclear group. Univariate analysis showed that there was no significant difference in tumor location, tumor diameter, macroscopic type, depth of invasion, histopathology, lesion characteristics (margin elevation, remarkable redness, uneven surface, ulcer), atrophy, intestinal metaplasia, or tumor markers (CEA, CA199, CA724) between the two groups (Table 2).

Histological measurements for the clear group and unclear group

A total of 81 pathological slices were obtained and analyzed in the lesion area of the clear group, focusing on 1,992 crypt structures while avoiding mucosal defect areas. In the lesion area of unclear group, 80 slices were examined, encompassing a total of 1,941 crypt structures. Comparing the histology of the lesion area between the unclear group and clear group, it was found that there were significant differences in crypt area (8108.46±7372.47 vs. 4169.76±4240.01 μm^2) ($P<0.0001$) (Fig. 3a), crypt length (206.06±135.09 vs. 125.69±97.56 μm) ($P<0.0001$) (Fig. 3b), crypt opening diameter (46.30±36.79 vs. 36.31±28.67 μm) ($P<0.0001$) (Fig. 3c). There was no significant difference in intercrypt distance between the two groups (79.91±53.36 vs. 78.11±63.11 μm) ($P=0.8024$) (Fig. 3d) (Table 3). There was a significant difference in the distribution of crypt structures between the two groups. The clear group was mainly characterized by fused crypts and absent crypts, while the unclear group was dominated by regular crypt structures (73.68%) (Fig. 3e).

The marginal normal area of the lesion encompassed the upper and lower incisal margins and the area outside the electrocoagulation mark of each tissue strip, as depicted in Fig. 4a. In the clear group, a total of 768 crypt structures were analyzed in the normal area. In the unclear group, 648 crypt structures were analyzed in the normal area. Comparing the histology of the cancer area and marginal normal area of the two groups, it was found that there were significant differences in crypt area (4169.76±4240.01 vs. 5815.22±5939.04 μm^2, $P=0.0003$), crypt length (125.69±97.56 vs. 170.34±132.32 μm, $P<0.0001$)), crypt opening diameter (36.31±28.67 vs. 56.05±42.72 μm, $P<0.0001$)), and intercrypt distance (78.11±63.11 vs. 85.73±70.15 μm, $P=0.1294$) in the clear group, but there was no significant difference in the unclear group. In addition, in the clear group, the crypt area, crypt length, and crypt opening diameter in the normal area were larger than those in the cancer area. (Fig. 4) (Table 3).

Discussion

Compared with traditional white light endoscopy, IC chromoendoscopy performs better not only in its higher detection rate for early gastric cancer lesions but also in the determination of the demarcation line. In this study, there were 79 lesions (42.25%) whose boundaries could not be determined by white light endoscopy, and more than half of them (54.43%) had clearly delineated boundaries after IC staining, which was similar to previous reports [4]. Nagahama, T. et al. [13] reported that the accuracy of IC staining for the determination of the boundary of EGC lesions was 85.7% (80.4–91.0%)

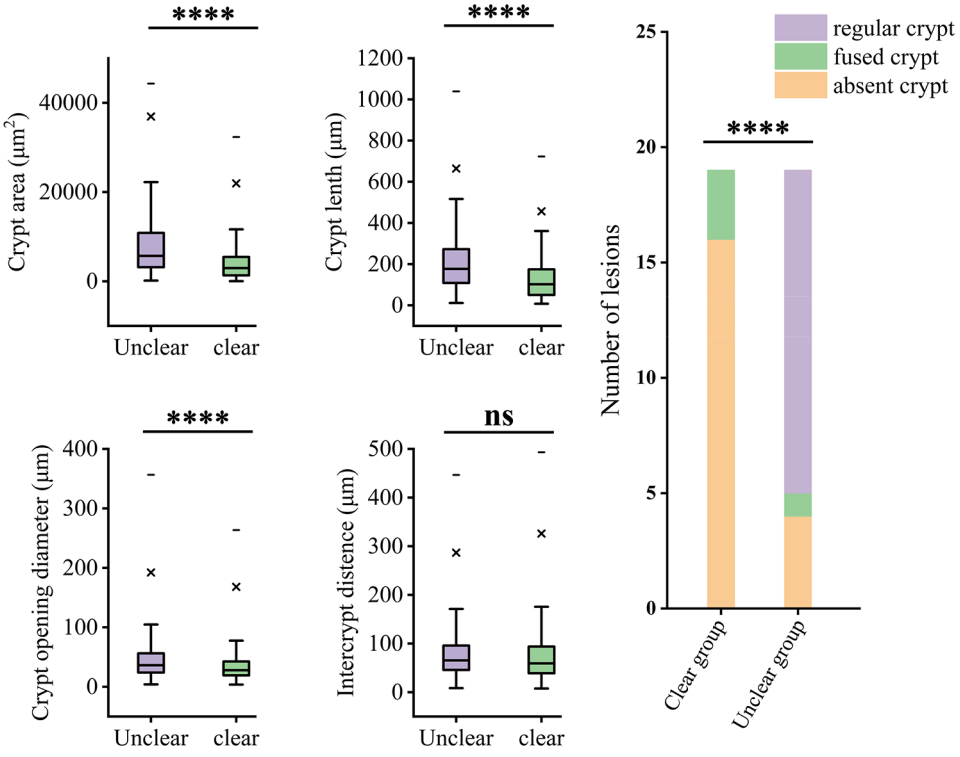

Fig. 3 Differences of crypt structure in cancer area between the clear group and unclear group. **a** Comparison of the crypt area; **b** Comparison of the crypt length; **c** Comparison of the crypt opening diameter; **d** Comparison of the intercrypt distance; e Comparison of the crypt structure. **** $P < 0.0001$; ns, not significant

Table 3 Histological data of the clear group and unclear group

	Unclear group		Clear group		*P* value		
	Cancer area	Normal area	Cancer area	Normal area	a	b	c
Crypt area (μm²)	8108.46 ± 7372.47	7945.07 ± 7618.46	4169.76 ± 4240.01	5815.22 ± 5939.04	< 0.0001	0.9585	0.0003
Crypt length (μm)	206.06 ± 135.09	200.34 ± 125.12	125.69 ± 97.56	170.34 ± 132.32	< 0.0001	0.7913	< 0.0001
Crypt opening diameter (μm)	46.3 ± 36.79	41.62 ± 30.59	36.31 ± 28.67	56.05 ± 42.72	< 0.0001	0.3362	< 0.0001
Intercrypt distance (μm)	79.91 ± 53.36	84.83 ± 56.37	78.11 ± 63.11	85.73 ± 70.15	0.8024	0.3168	0.1294

Note a is the comparison of cancer area between the clear group and unclear group. b is the comparison between the cancer area and the normal area in the unclear group. c is the comparison between the cancer area and the normal area in the clear group

by placing a marking dot on the most proximal margin. Moreover, this multicenter, randomized, controlled study also revealed that there was no significant difference between IC chromoendoscopy and ME-NBI in terms of the accuracy of delineation of gastric tumors before the ESD procedure. It seemed that IC chromoendoscopy could determine the horizontal boundary for most EGC lesions. Therefore, it is important to clarify the applicable conditions of indigo carmine staining to improve the complete removal rate of the lesions.

Previous studies on the applicable conditions of chromoendoscopy for the boundary of EGC were mainly focused on acetic acid combined with indigo carmine staining (AI). Lee, B.E. et al. [14] and Hong, S.M. et al. [7] reported that lesion histology was an independent risk factor affecting the clarity of the lesions after AI chromoendoscopy, and undifferentiated lesions showed a higher frequency of mottled appearance than differentiated adenocarcinomas. Numata, N. et al. [15] found that compared with the white light endoscope, the advantage of AI chromoendoscopy is mainly reflected in protruded or flat elevated-type EGC or at the atrophic border on the oral side of EGCs. Researchers evaluated the determination of the margin of EGC lesions by using simple IC staining and found that normal mucosal color, 0-IIb lesions, lesions larger than 21 mm, ulcers, and components of poorly differentiated adenocarcinoma were the risk factors that make the determination of the margin difficult [16]. Unlike previous studies, in the present study, although the rate of indistinct borders was higher in undifferentiated lesions, there was no significant difference compared with differentiated adenocarcinoma. The reason may be that there were fewer undifferentiated lesions in the present study. Another possible explanation

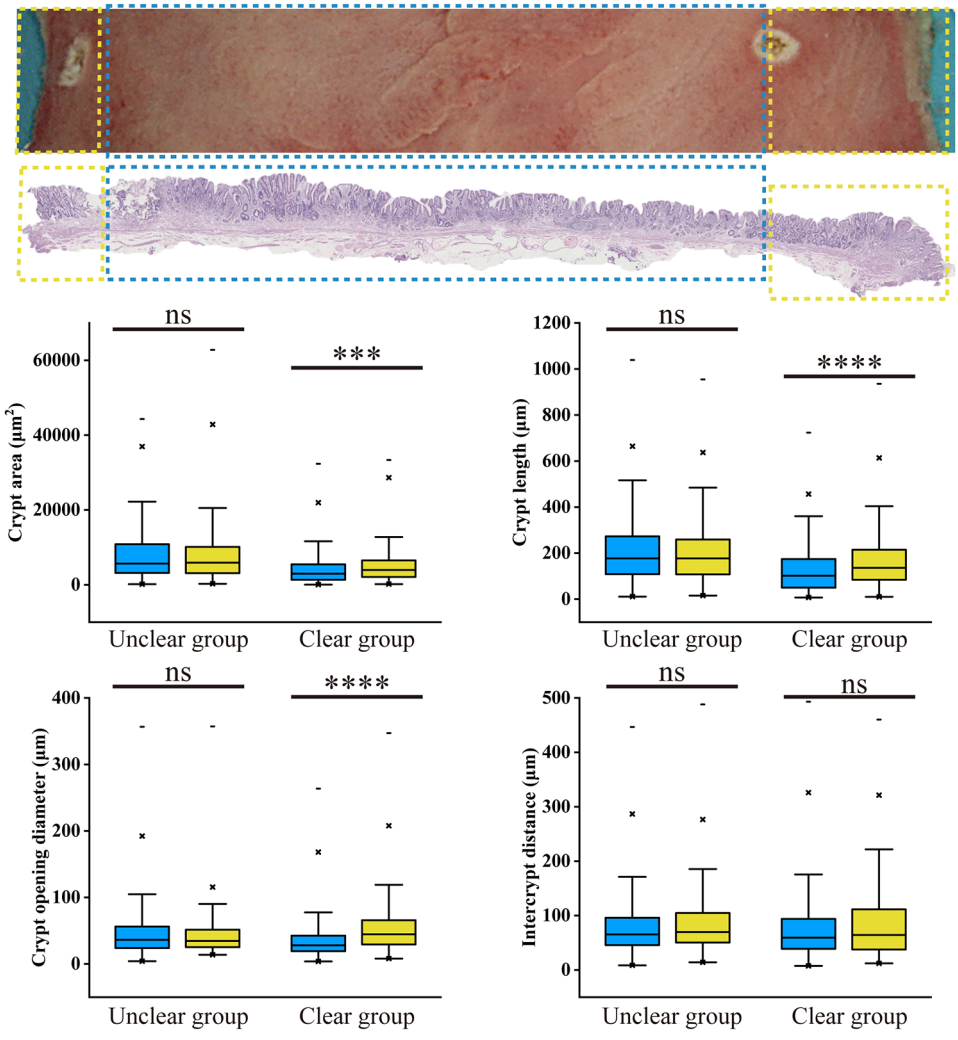

Fig. 4 Comparison of histology between the cancer area and marginal normal area. **a** Tissue slice obtained from the samples: the yellow area outside the marked point is the marginal normal area, and the blue area in the marked point is the cancer area. **b** Corresponding pathological image of the tissue slice: The yellow area outside the marked point is the marginal normal area, and the blue area inside the marked point is the cancer area. **c** Comparison of histology between the normal area and cancer area of the clear group and unclear group. c1 Comparison of the crypt area; c2 Comparison of the crypt length; c3 Comparison of the crypt opening diameter; c4 Comparison of the intercrypt distance. Cancer area: blue box plots; Normal area: yellow box plots; ns, not significant; *** $P < 0.001$; **** $P < 0.0001$

is that gastric cancer tissue usually exhibits histological heterogeneity, and the same lesion may contain multiple cells with different degrees of differentiation, whereas most of the lesions in this study were focal poorly differentiated lesions in a highly differentiated background. In addition, Nagahama et al. [13] also reported that in the group with unclear lesion boundaries, the most common histological type of inaccurately delineated lesions was not simply the undifferentiated type, but rather the undifferentiated type adenocarcinoma infiltrating the glandular neck zone covered with non-neoplastic epithelium.

In addition, by analyzing and comparing the crypt structures of lesions between the clear group and unclear group, we found that the clear group mainly consisted of lesions with fused or absent crypt structures, while the unclear group consisted of lesions with regular crypt structures. By measuring the structure of the crypt in the lesion area, it was found that compared with the unclear group, the crypt area was smaller, the crypt opening diameter and the length of the crypt was shorter in the clear groups. Comparing the crypt structure of the cancer area and the paracancerous normal area of the two groups, we found that in the clear group, the crypt opening area was larger, the opening diameter was wider, and the crypt length was longer in the paracancerous normal region than in the cancer region. In the unclear group, there was no significant difference in crypt area, crypt length, crypt opening diameter, or intercrypt distance between the two regions. It is thus evident that the determination of the lesion border by indigo carmine

staining was greatly related to the epithelial histomorphology, which is consistent with the staining principle of IC. Normal gastric mucosa deposits dye uniformly due to its regular crypt surface structure. Lesions with fused or absent crypt structures, small crypt areas, short crypt lengths, short crypt opening diameters, and large intercrypt distances show a clear DL because they cannot uniformly deposit indigo carmine dye. This irregular surface structure is in sharp contrast to normal mucosa. Conversely, lesions with regular crypt structures can still deposit dye uniformly on their surface, making these lesions indistinguishable from the surrounding normal mucosa. Although no identical studies exist to confirm these results, a study examining the histological structure of gastric epithelial tumors and microsurface patterns (MSPs) observed through magnification endoscopy found a close relationship between the crypt structure and MSPs. It found that lesions without MSPs have a lower crypt opening density, shorter crypt length, greater intercrypt distance, and larger crypt angle [12, 17]. This finding supports the results of our study to some extent. Therefore, we predicted that dyes were likely not easily deposited onto lesions with absent MSPs in ME-NBI during indigo carmine staining and that such lesions were easily distinguished from the surrounding normal mucosa. However, large-scale prospective studies are needed for verification. Nonetheless, the current evidence underscores the importance of mucosal surface microstructure, particularly in endoscopy. While it may be challenging for pathologists to measure the parameters related to each crypt's structure in detail during their routine work, our findings suggest a significant insight: pathologists should consider the relevant characteristics of the mucosal surface crypt structure in addition to the usual assessments of lesion nature and infiltration depth. Specifically, lesions with deep structures containing signet-ring cells or other undifferentiated cells but regular mucosal surface crypt structures pose a diagnostic challenge. For such lesions, it is difficult to accurately determine the boundary range using either chromoendoscopy or ME-NBI. However, enhanced communication between endoscopists and pathologists regarding these crypt structure characteristics could help avoid incomplete resections and lead to better treatment plans for patients.

There are some limitations in this study. First, we could not evaluate the preoperative preparation. The presence of mucus and foam in the stomach might have a certain impact on the staining of indigo carmine. However, in addition to the preoperative defoamer, poorly prepared patients will be given a defoamer again to ensure accurate assessment of the lesions. Second, this study was retrospective, and the evaluation of the staining effect was only based on endoscopic reports and images in the endoscopic system, lacking the dynamic process during staining. To address the limitations of the study, a future prospective study is planned so that preoperative preparations can be controlled and overall evaluation of the staining effect can be performed to ensure the reliability of the results.

Conclusions

In conclusion, 80.75% of lesions were found to have clear lesion borders by IC chromoendoscopy. The crypt structure was the main influencing factor in the assessment of lesion borders by IC staining. Lesions with fused or absent crypt structures, a small crypt area, a short crypt length, a short crypt opening diameter can be used to easily determine the margin by IC chromoendoscopy.

Abbreviations

EGC	Early gastric cancer
IC	Indigo carmine
DL	Demarcation line
ESD	Endoscopic submucosal dissection
WLE	White light endoscopy
ME-NBI	Magnifying endoscopy with narrowband imaging
HE	Hematoxylin and eosin
CEA	Carcino-embryonic antigen
CA199	Carbohydrate antigen199
CA724	Carbohydrate antigen724
IM	Intestinal metaplasia
AI	acetic acid combined with indigo carmine staining MSPs Microsurface patterns

Acknowledgements

We acknowledge the participating hospitals for their assistance.

Author contributions

JW, NL, and BQ designed the study. BQ and NL obtained the funding for this study. XJ and YZ collected the data. BQ, LD, and BZ reviewed the literature. XJ, LQ and YH analysed and interpreted the data; XJ, LQ and QY interpreted the results and wrote the manuscript. All authors have read the manuscript.

Funding

This work was supported in part by the Key Research and Development Projects of Shaanxi Province under Grants 2024SF-YBXM-109 and 2022SF-065.

Data availability

The data involved in this study are available from the corresponding author upon reasonable request.

Declarations

Ethics approval and consent to participate

All methods were performed in accordance with the Declaration of Helsinki. This study was approved by the Medical Ethics Committee of the Second Affiliated Hospital of Xi'an Jiaotong University (2021196). This study collected data from hospital medical records from the period of January 2015 until March 2023, and it is not feasible to find all the patients who received ESD during these periods and have them sign the consent form. Furthermore, this study neither contains personal information nor involves commercial interests. Thus, the requirement for informed consent was waived during ethical applications (Medical Ethics Committee of the Second Affiliated Hospital of Xi'an Jiaotong University). The patient information was kept confidential, and the results of the study were reflected in the form of group data analysis.

Consent for publication

Not applicable.

Competing interests
The authors declare no competing interests.

Received: 4 December 2023 / Accepted: 6 August 2024
Published online: 15 August 2024

References

1. Suzuki H, Oda I, Sekiguchi M, Abe S, Nonaka S, Yoshinaga S, et al. Factors associated with incomplete gastric endoscopic submucosal dissection due to misdiagnosis. Endosc Int Open. 2016;4:E788–793. https://doi.org/10.1055/s-0042-108191.
2. Kim TK, Kim GH, Park DY, Lee BE, Jeon TY, Kim DH, et al. Risk factors for local recurrence in patients with positive lateral resection margins after endoscopic submucosal dissection for early gastric cancer. Surg Endosc. 2015;29:2891–8. https://doi.org/10.1007/s00464-014-4016-6.
3. Ono H, Yao K, Fujishiro M, Oda I, Uedo N, Nimura S, et al. Guidelines for endoscopic submucosal dissection and endoscopic mucosal resection for early gastric cancer (second edition). Dig Endosc off J Jpn Gastroenterol Endosc Soc. 2021;33:4–20. https://doi.org/10.1111/den.13883.
4. Yoshinaga S, Oda I, Abe S, Nonaka S, Suzuki H, Takisawa H et al. Evaluation of the margins of differentiated early gastric cancer by using conventional endoscopy. World J. Gastrointest. Endosc. 2015;7:659–664. https://doi.org/10.4253/wjge.v7.i6.659.
5. National Health Commission. Standards for diagnosis and treatment of gastric cancer (2018) [J]. Chinese Journal of Digestion and Medical Imageology, 2019;9(3): 118–144.
6. Ida K, Hashimoto Y, Takeda S, Murakami K, Kawai K. Endoscopic diagnosis of gastric cancer with dye scattering. Am J Gastroenterol. 1975;63(4):316–20. PMID: 48340.
7. Hong SM, Kim GH, Lee BE, Lee MW, Kim DM, Baek DH, et al. Association between mucin phenotype and lesion border detection using acetic acid-indigo carmine chromoendoscopy in early gastric cancers. Surg Endosc. 2022;36:3183–91. https://doi.org/10.1007/s00464-021-08626-4.
8. Yao K, Oishi T, Matsui T, Yao T, Iwashita A. Novel magnified endoscopic findings of microvascular architecture in intramucosal gastric cancer. Gastrointest Endosc. 2002;56(2):279–84. https://doi.org/10.1016/s0016-5107(02)70194-6.
9. Yao K, Anagnostopoulos GK, Ragunath K. Magnifying endoscopy for diagnosing and delineating early gastric cancer. Endoscopy. 2009;41(5):462–7. https://doi.org/10.1055/s-0029-1214594.
10. The Paris endoscopic classification of superficial neoplastic. Lesions: esophagus, stomach, and colon: November 30 to December 1, 2002. Gastrointest Endosc. 2003;58:S3–43. https://doi.org/10.1016/s0016-5107(03)02159-x.
11. WHO Classification of Tumours Editorial Board. WHO classification of tumours of digestive system [M]. 5th ed. Lyon: IARC P ress; 2019. p. 60.
12. Chuman K, Yao K, Kanemitsu T, Nagahama T, Miyaoka M, Takahashi H, et al. Histological Architecture of gastric epithelial neoplasias that showed absent microsurface patterns, visualized by magnifying endoscopy with narrow-Band Imaging. Clin Endosc. 2021;54:222–8. https://doi.org/10.5946/ce.2020.090.
13. Nagahama T, Yao K, Uedo N, Doyama H, Ueo T, Uchita K, et al. Delineation of the extent of early gastric cancer by magnifying narrow-band imaging and chromoendoscopy: a multicenter randomized controlled trial. Endoscopy. 2018;50:566–76. https://doi.org/10.1055/s-0044-100790.
14. Lee BE, Kim GH, Park DY, Kim DH, Jeon TY, Park SB, et al. Acetic acid-indigo carmine chromoendoscopy for delineating early gastric cancers: its usefulness according to histological type. BMC Gastroenterol. 2010;10:97. https://doi.org/10.1186/1471-230X-10-97.
15. Numata N, Oka S, Tanaka S, Yoshifuku Y, Miwata T, Sanomura Y, et al. Useful condition of chromoendoscopy with indigo carmine and acetic acid for identifying a demarcation line prior to endoscopic submucosal dissection for early gastric cancer. BMC Gastroenterol. 2016;16:72. https://doi.org/10.1186/s12876-016-0483-7.
16. Sakai Y, Eto R, Kasanuki J, Kondo F, Kato K, Arai M, et al. Chromoendoscopy with indigo carmine dye added to acetic acid in the diagnosis of gastric neoplasia: a prospective comparative study. Gastrointest Endosc. 2008;68:635–41. https://doi.org/10.1016/j.gie.2008.03.1065.
17. Yagi K, Nozawa Y, Endou S, Nakamura A. Diagnosis of early gastric Cancer by magnifying Endoscopy with NBI from viewpoint of histological imaging: mucosal patterning in terms of White Zone Visibility and its relationship to histology. Diagn Ther Endosc. 2012;2012:954809. https://doi.org/10.1155/2012/954809.

Publisher's Note